Lawrence Berkeley Laboratory
UNIVERSITY OF CALIFORNIA

Presented at the Workshop on Collective States in Nuclei, Suzhou University, China, September 8-18, 1983; and to be published in the Proceedings

NUCLEAR MOMENTS OF INERTIA AT HIGH SPINS

M.A. Deleplanque

December 1983

Prepared for the U.S. Department of Energy under Contract DE-AC03-76SF00098

DISCLAIMER

LBL-17082

NUCLEAR MOMENTS OF INERTIA AT HIGH SPINS

M. A. DELEPLANQUE

Nuclear Science Division, Lawrence Berkeley Laboratory, University of California, Berkeley, CA 94720, U.S.A.

Nuclei with highest angular momentum are discussed. The production of high spin states, and the basic ideas associated with high spin physics are reviewed. Recent developments from "continuum" γ-ray studies are presented: the measurement of different average moments of inertia gives new information on the interplay between collective and single particle aspects at high spins. Finally, the exciting possibility of resolving the "continuum" spectra with new detector systems is examined.

1. INTRODUCTON

Angular momentum is a dimension along which nuclear properties can be examined. Just as information on deformation and shell effects came from studying a series of nuclei, the properties of the nuclei for a series of spins will show its response to new forces, namely Coriolis and centrifugal, which are large. Also the highest spin studies I shall consider here separate from the more conventional "discrete γ-ray spectroscopy" since we have to deal with average properties measured on "continuum γ-ray spectra." This report will show recent progress made in identifying specific orbital effects and shape effects at the highest spins. It will also emphasize the exciting possibilities offered by the new generation of detectors, especially large arrays of Compton-suppressed germanium detectors.

2. PRODUCTION OF THE HIGHEST SPIN STATES

2.1. Spin limit

At very high angular momentum, the nucleus tends to fission. This will limit the spin values at which nuclear structure can be observed through γ-ray decay. The liquid drop model, which reproduces well the gross average properties of the nucleus, estimates this limiting spin[1] (Figure 1). The angular momentum at which the fission barrier is 8 MeV is plotted (dashed line) as a function of nucleon number for nuclei along the stability line: since in the fission process, a lot of angular momentum is tied up in the relative motion of the fragments and not in the nucleus itself, particle evaporation must effectively compete with fission in order to leave high spin in the residual nuclei. This is empirically found to happen for a fission barrier

greater than 8 MeV. For the heavier nuclei, neutrons are most often emitted, and they carry very little angular momentum. For the lighter nuclei, where the Coulomb barrier decreases, α particles are preferentially emitted and they can carry a lot of angular momentum, limiting further the highest spin attainable[2] (dotted line). Thus, the maximum spins produced are around 70 $\hbar$ and are located in the rare earth region (A ~ 150). This is the region I'll discuss here.

2.2. Production of high spin states

A compound nucleus is formed at high excitation energy (~80 MeV) and the angular momentum distribution $\sigma(I)$ for the evaporation residues is roughly triangular (σ proportional to $2I + 1$) up to the maximum spin. The excitation energy is most often carried away by a few neutrons down to one neutron binding energy (~8 MeV) above the yrast line. Below that level, called the "entry limit," γ-ray emission is predominant. This is the region of nuclear structure studies, as shown in Figure 2, on an excitation energy versus spin plot. Two kinds of γ-rays deexcite the nucleus: i) the "statistical" γ-rays[3]

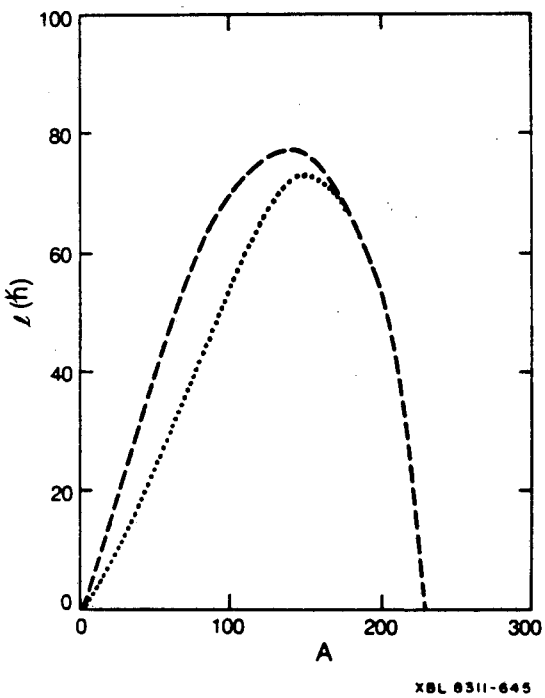

FIGURE 1
Rotating liquid drop calculation of the angular momentum at which the fission barrier is 8 MeV (dashed line). The dotted line is an experimental estimate of the angular momentum below which γ-rays are emitted.

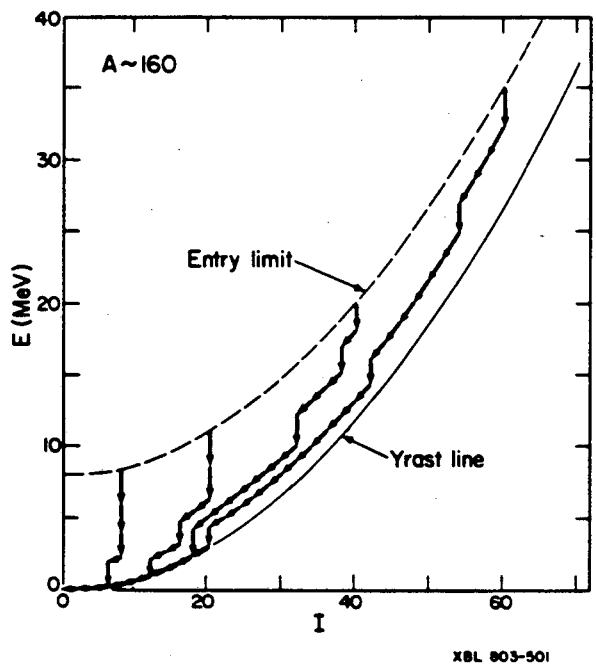

FIGURE 2
Typical γ-ray deexcitation paths. Vertical arrows indicate statistical transitions. Arrows parallel to the yrast line represent yrast-like transitions.

remove the energy (vertical arrows). They are fast and their lifetime is approximately independent of spin. ii) The "yrast-like" γ-rays remove the angular momentum (arrows parallel to the yrast line). Most often, and in particular in rotational nuclei considered here, they are the collective stretched E2 transitions. Their energy E_γ increases with spin, and their transition probability, proportional to E_γ^5, increases with spin. At low spin they are slower than the statistical transitions, so that the population is concentrated on the yrast line. But above spin around 40 $\hbar$ the two kinds of transitions compete, which results in many different paths for the nucleus. Individual lines are no longer separable and we detect an "unresolved" or "continuum" γ-ray spectrum.

2.3. Detection of high spin states

Those two kinds of γ-ray are separable on a continuum γ-ray spectrum. Figure 3 shows such a spectrum obtained from a (12.7 x 15 cm) NaI scintillator, which has a poor resolution but a rather good peak to total ratio (~50%), so that the spectrum can be reasonably well unfolded. From its exponential tail, a "statistical" spectrum can be subtracted (dashed line). The remaining "yrast" part of the spectrum contains most of the nuclear structure information.

3. BASIC IDEAS SPECIFIC TO HIGH SPINS

The nucleus is a many-body system and therefore will have some macroscopic "classical" properties. But it is also a quantal system of finite size, so that the classical properties will be modified by quantal effects which sometimes single out some particular orbital.

3.1. Nuclear shapes

3.1.1. Classical shapes

The low-lying excitations correspond to the rotational degree of freedom. We shall neglect the pairing correlations which are expected to be quenched at high spins. Classically, the most favored shape will be that which minimizes the rotational energy of a rigid body, or maximizes its moment of inertia. If an axially symmetric nucleus is considered, for example, the shape is characterized by the parameter $\beta \approx \Delta R/R$, the difference in radius along 2 axes divided by the average radius. The optimum conditions correspond to an oblate (disc-like) nucleus rigidly rotating around its symmetry axis (OS). The next lowest energy is that of a prolate (cigar-like) nucleus rotating around an axis perpendicular to the symmetry axis ($P_\perp$). The other two possibilities are $O_\perp$ and PS.

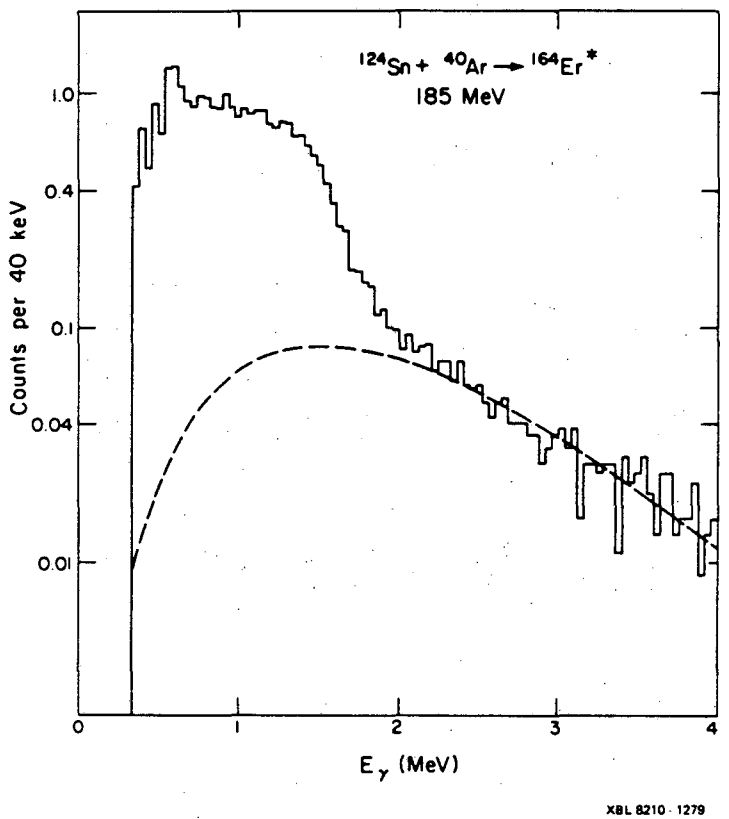

FIGURE 3
Isotropic γ-ray spectrum (histogram), normalized to the γ-ray multiplicity, from the deexcitation of high spin states of the compound nucleus ^{164}Er. Its statistical part is shown as a dashed line.

3.1.2. Quantal effects

As a quantal system, the nucleus has a shell structure, which in turn depends on its shape. At low spin, those "shell effects" and the pairing correlations can reverse the classical order of shapes. At high spins, the shell effects[4] (of order 3-4 MeV) are small enough that the two highest, trajectories ($O_\perp$ and PS) can be ignored. They can, however, change the order of the lowest two (OS and $P_\perp$). More exact calculations (like the cranking model) also give the same results. In addition, they also show that nuclei near major shells tend to be oblate or spherical, nuclei near the middle of a shell tend to be prolate. The classical picture is also perturbed by another property of a quantal object: it cannot rotate around its symmetry axis. But Bohr and Mottelson have shown[5] that, on average, the energy of such a system is the same as if it <u>were</u> rigidly rotating around that axis, so that the conclusion drawn above is still valid. For that reason, the behavior of such a system is called an "effective" rotation around its symmetry axis. But the characteristics of its γ-ray deexcitation are very different from those of a good rotor: the transitions are non-collective, irregular and can be of

dipole or quadrupole type. These properties are just a result of the fact that such a motion is contained in the single-particle degrees of freedom. For a nucleus rotating around an axis perpendicular to the symmetry axis, the rotation is collective and gives rise to regular "rotational" bands of collective stretched E2 transitions E_γ. They define the "rotational frequency" ω which is approximately equal to $E_\gamma/2$. The frequency cannot be measured experimentally for a non-collective nucleus, but the notion of effective rotation is behind the extension of the cranking model to the non-rotating nuclei. The frequency is then a parameter: the nuclear potential is rotated with a frequency ω either around the symmetry axis or around an axis perpendicular to the symmetry axis. Properties of the nucleus--total energy, spin--can then be calculated as a function of frequency, and in most cases can be compared with experiment (when ω can be measured). The rotational frequency is presently considered as a new dimension along which many nuclear properties calculated and measured.

3.2. Interplay between collective and single particle effects

Even rotational nuclei do not rotate like a rigid body. This happens because the Coriolis force is strongest for the orbitals of highest angular momentum j. The Coriolis force tends to align the particle angular momentum j on the rotation axis, thereby decoupling its motion from that of the rest of the nucleus. The collectivity therefore decreases. This is the first step towards the non-collective situation described above. All intermediate situations are possible and characterized by the parameter γ which varies from 0° for the collective case (P_1) to 60° for the non-collective behavior (OS).

In general there are two kinds of contributions to the angular momentum as shown on Figure 4 for ^{158}Er. The smooth regular increase in spin comes from the collective motion. The sharp increase at $\hbar\omega \approx 0.28$ MeV and in the spin region 10-16 is due to the alignment of a pair of neutrons (in this case $\nu i_{13/2}$) on the rotation axis. This is the single-particle contribution to the angular momentum. The region of spin between 16^+ and 24^+ thus represents a collective band constructed on a ($\nu i_{13/2}$) two-quasiparticle states. The change i in the nuclear alignment at that crossing is approximately the difference between the spins in the two "unperturbed" bands at a given frequency.

The frequency of the crossing is characteristic of the orbitals involved. In a cranking model diagram, which shows single particle energies in the rotating frame as a function of frequency, this corresponds to the crossing of two orbitals: two-quasiparticle orbitals at low spins, or two single-particle

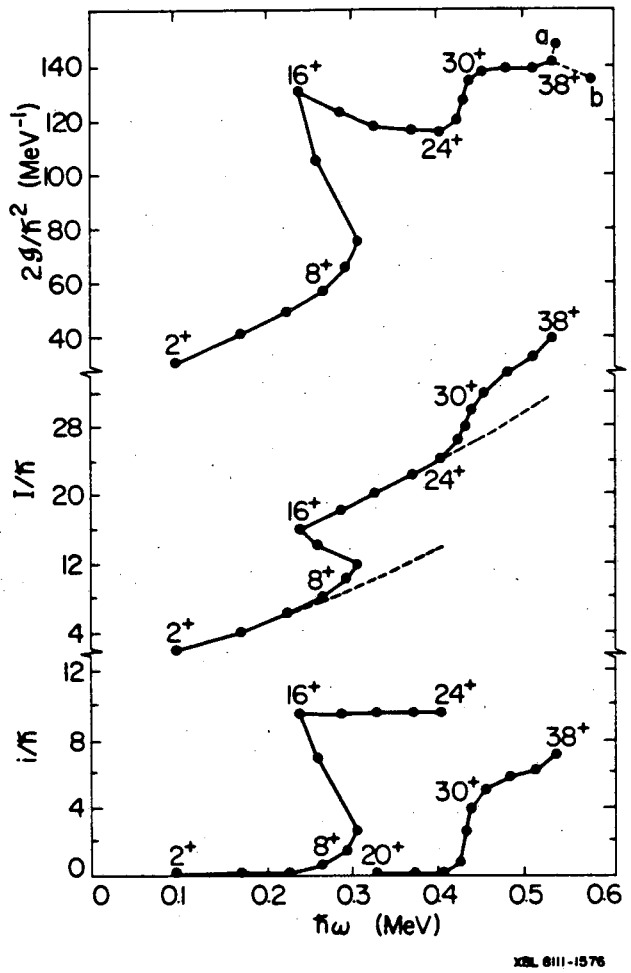

FIGURE 4
Plots of the moment of inertia $\mathcal{I}^{(1)}_{eff}$, of the total spin I, and of the alignment i as a function of frequency for the nucleus ^{158}Er.

orbitals at high spins where the pairing correlations are neglected. Figure 5 gives such a diagram for protons around mass 165. The alignment is the slope of those orbitals. Near Z=66, there are only a few downsloping (aligned) orbitals, mainly 541 1/2 ($h_{9/2}$) and 660 1/2 ($i_{13/2}$), and they reach the Fermi level at a frequency close to 0.6 MeV. In that mass region this frequency corresponds to a spin around 45 ħ, i.e., in the region where the γ-ray spectra are unresolved and many bands deexcite the nucleus. Schematically, one expects that those aligned orbitals become populated in essentially all the bands around $\hbar\omega \simeq 0.6$ MeV. But since all these bands would differ by the rest of the configuration, it is not clear whether these many crossing frequencies would be similar enough to permit identification of the aligning orbital. This is still an open question.

3.3. Collective and effective moments of inertia

Since we cannot resolve individual bands at high spins, we cannot identify

band crossings as shown in Figure 4. This question must be addressed differently, through the notion of moments of inertia.

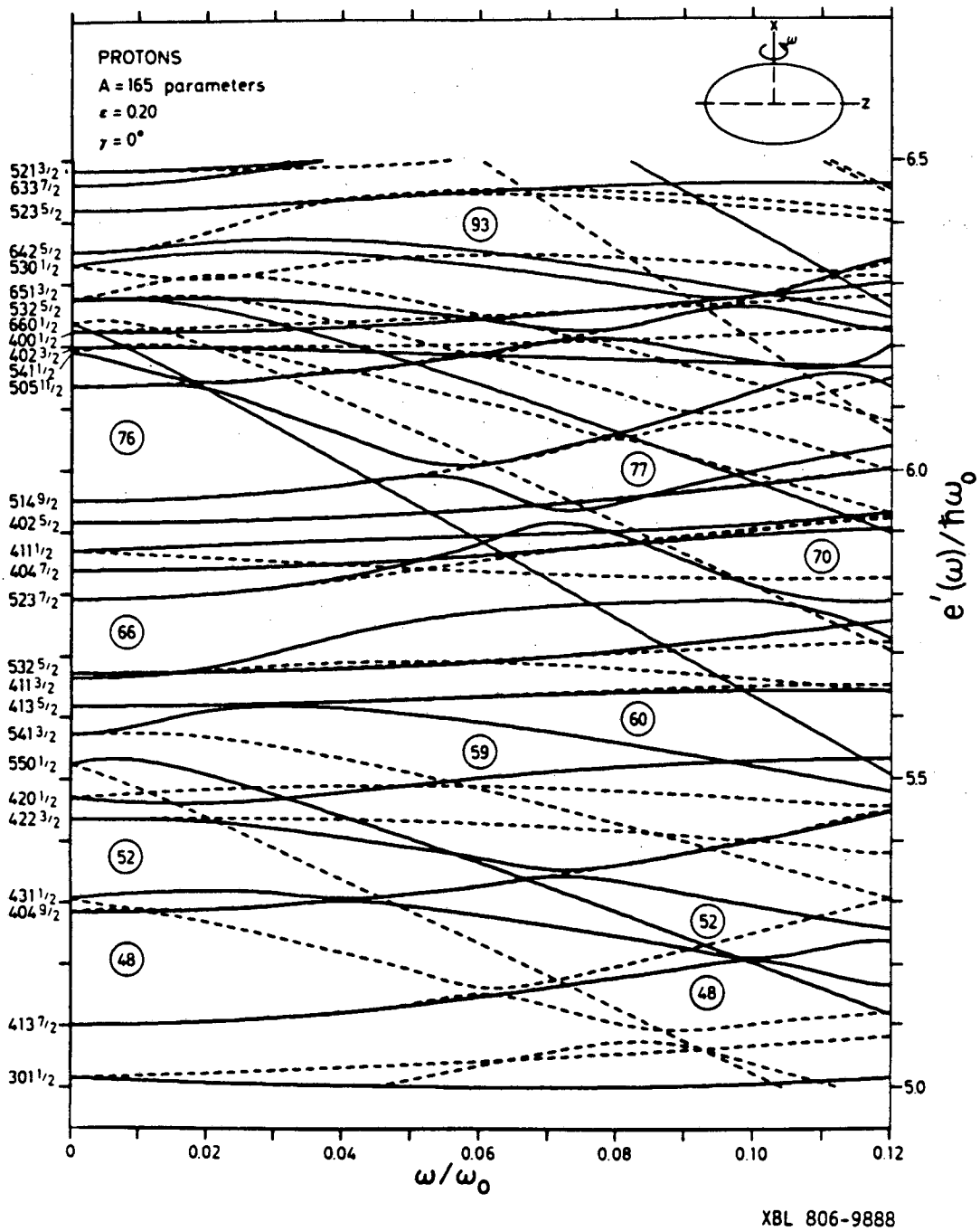

FIGURE 5
Example of energy levels as a function of rotational frequency (in units of oscillator frequency ω_0) calculated with a cranked modified oscillator potential (from Ref. 7). The solid and dashed lines correspond to states of different signatures.

They are of two kinds: the kinematic moments of inertia, which are related to the overall motion of the nucleus, and the dynamic moments of inertia, which

describe its response to the torque. For a perfect rotor with a moment of inertia $\mathcal{J}$, the rotational energy at spin I is $E \approx \hbar^2 I^2/2\mathcal{J}$. Its first derivative with respect to spin: $dE/dI = \hbar^2 I/\mathcal{J} = E_\gamma/2 = \hbar\omega$, is related to the kinematic moment of inertia $\mathcal{J}^{(1)}$ defined as $\mathcal{J}^{(1)}/\hbar^2 = I(dE/dI)^{-1} = I/\hbar\omega$. The second derivative $d^2E/dI^2 = \hbar^2/\mathcal{J} = \hbar d\omega/dI$ is related to a dynamic moment of inertia $\mathcal{J}^{(2)}$: $\mathcal{J}^{(2)}/\hbar^2 = (d^2E/dI^2)^{-1} = dI/\hbar d\omega$. $\mathcal{J}^{(2)}$ represents the rate of change in spin with frequency. Those two moments of inertia are identical for a perfect rotor. But when there are changes in the internal structure of the nucleus, such as alignment of single-particle angular momentum, I/ω will be different from $dI/d\omega$ reflecting the fact that the nuclear motion is not the simple rotation of a rigid body. The moment of inertia $\mathcal{J}^{(1)}$ at a frequency ω is an average of $\mathcal{J}^{(2)}$ over a frequency region from 0 to ω and therefore will be much less sensitive to variations with frequency. We will therefore concentrate on the determination of dynamic moments of inertia $\mathcal{J}^{(2)}$.

Those moments of inertia can be defined for any sequence of levels, but two of them play an important role in the decay modes of the nucleus. The characteristic feature of collective motion is the rotational band (see Figure 4). It is therefore natural to define a moment of inertia $\mathcal{J}^{(2)}_{band} = (dI/d\omega)_{band}$ by calculating $dI/d\omega$ only in the band region. Provided the alignment and the deformation are reasonably constant within a band, $\mathcal{J}^{(2)}_{band}$ is related to the collectivity of the motion. If $dI/d\omega$ is considered for a whole decay path, both collectivity and alignment will be taken into account and therefore an effective moment of inertia is defined by $\mathcal{J}^{(2)}_{eff} = (dI/d\omega)_{path}$. For a single decay path $\mathcal{J}^{(2)}_{eff} = \mathcal{J}^{(2)}_{band}$ in the band regions, but $\mathcal{J}^{(2)}_{eff}$ can become very large in the regions of alignment (band crossing).

Both $\mathcal{J}^{(2)}_{band}$ and $\mathcal{J}^{(2)}_{eff}$ can be calculated as a function of frequency in the cranking model and measured experimentally. However the measured values represent an average over many decay paths and therefore will probably be smeared as compared to the theory. Nevertheless, the comparisons should be very useful since they are at present the only contact between theory and experiment.

4. EXPERIMENTAL DETERMINATION OF MOMENTS OF INERTIA AT HIGH SPINS

4.1. Selection of high spin states

Because the γ-rays are emitted in a limited domain (extending from 0 to ~ 8 MeV, see Figure 2) above the yrast line, the total γ-ray energy is related to the initial spin. Therefore high spin states are selected by a high total

γ-ray energy E_{tot}. E_{tot} is measured in a high efficiency device: it can be two large NaI scintillators, or a "ball" composed of many scintillators. In coincidence with those, the γ-ray spectra are obtained in a number of γ-ray detectors, placed at different angles. They are far away from the target to avoid pile-up effects and to discriminate against neutrons by time of flight.

4.2. Determination of $\mathcal{J}^{(2)}_{band}$

The rotational band structure is easily recognizable on a γ-γ coincidence plot (Figure 6). It shows a "valley" along the main diagonal (no two γ-rays have the same energy) and a "ridge" structure. The width of the valley is just $4dE_\gamma/dI = 8\ d\omega/dI = 16\ \hbar^2/2\mathcal{J}^{(2)}_{band}$. We measure $\mathcal{J}^{(2)}_{band}$ because only in-band transitions will give rise to that regular structure. If many bands have the same moment of inertia, the intensity will appear on the same

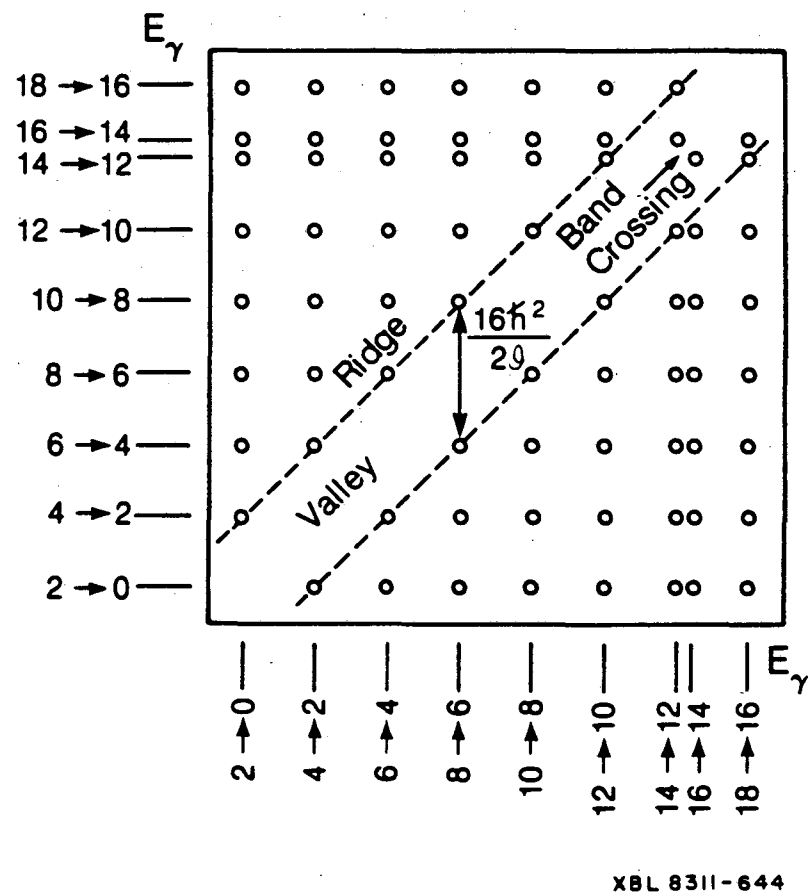

FIGURE 6
Idealized γ-γ correlation pattern for a perfect rotor with a band crossing at spins 14-16 $\hbar$.

ridges. Therefore, even without resolving the bands, their moment of inertia can be measured. If there were a band structure at high spins, but with a variety of moments of inertia values, the ridges would be smeared out but the valley should still be visible. The band crossings tend to fill the valley at the crossing frequency (see Figure 6). But if the crossing frequencies in each band are sufficiently similar, they should show up as a distinct peak in the valley.

The results of such measurements are still tentative, because of experimental difficulties to obtain good statistics. The poor resolution of NaI scintillators (50 KeV at 1 MeV) tends to smear out the ridges too much so that the valley width is not well defined (it is ~100 KeV in the rare-earth region). Germanium detectors however have a bad peak/total ratio (~15%) so that about 98% of all events has to be removed as background. Great progress will surely be made when large arrays of Compton-suppressed germanium detectors are operational. At present the results are somewhat contradictary. In some rare earth nuclei[6], $\mathcal{J}^{(2)}_{band}$ seems to decrease at high frequency, as would be expected if additional alignments occur at high spins, and as some calculations seem to indicate. However, data from Daresbury[7] on ^{130}Ce (the first obtained with six Compton-suppressed Ge detectors) do not indicate a decrease of $\mathcal{J}^{(2)}_{band}$ at high frequencies.

4.3. Determination of $\mathcal{J}^{(2)}_{eff}$

A new--more quantitative--viewpoint on continuum γ-ray spectra was reached recently when it was recognized[8] that the height dN of a continuum γ-ray spectrum (normalized to the γ-ray multiplicity) is proportional to $\mathcal{J}^{(2)}_{eff}$ for a spectrum composed of collective stretched E2 transitions. If dE_γ is the channel width, the quantity $dN/dE_\gamma = dI/4d\omega$. Since there is no selection of in-band transitions in that spectrum, this is just $\mathcal{J}^{(2)}_{eff}/4$. $\mathcal{J}^{(2)}_{eff}$ describes how efficiently the angular momentum is generated at a given frequency. The most efficient way is probably the alignment, which occurs because it is a cheap way for the nucleus to generate angular momentum. It appears as a peak in a γ-ray (or $\mathcal{J}^{2}_{eff}$) spectrum, since several transitions are closer in energy.

There is an experimental problem in determining $\mathcal{J}^{(2)}_{eff}$ at high frequencies. These frequencies correspond to the highest spin states which, in a given total energy gate, are only partially fed. The height of the γ-ray spectrum in that region is then $\mathcal{J}^{(2)}_{eff}$ times the fraction of the population going through that spin (or frequency) region. We have devised a method to correct for that incomplete feeding for quasirotational spectra.

This method is most easily understood for a perfect rotor ($\mathcal{J}^{(2)}_{eff}(\omega)$ constant). The corresponding γ-ray spectrum would drop at high frequency because of the incomplete feeding at high spins, and the feeding (direct population) would just be its derivative. In practice, we obtain the feeding by taking a finite difference between two spectra corresponding to two slightly different populations selected by two slightly different total γ-energy slices.

Figure 7 shows an example of the results obtained for several Erbium nuclei. ^{160}Er is a rather good rotor showing a rather flat spectrum, except for the known first ($\hbar\omega \sim 0.28$ MeV), blocked and second ($\hbar\omega \sim 0.45$ MeV) backbends, and a rise at the highest ($\hbar\omega > 0.6$ MeV) frequencies. This rise is accompanied by a decrease in $\mathcal{J}^{(2)}_{band}$ (measured from a γ-γ correlation experiment), which

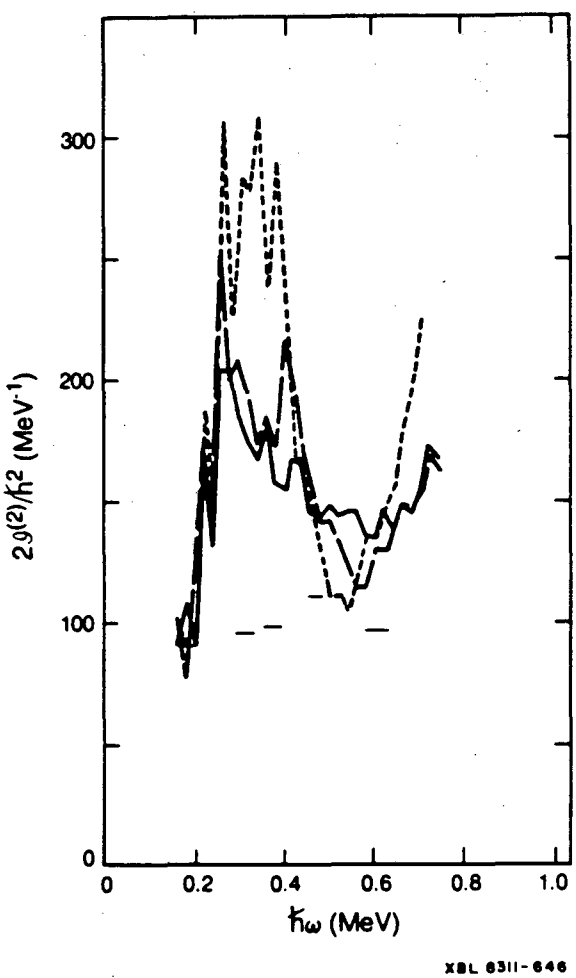

FIGURE 7
Plot of $\mathcal{J}^{(2)}_{eff}$ (thick lines) as a function of frequency for the systems ^{124}Sn + ^{40}Ar (solid line), ^{122}Sn + ^{40}Ar (long-dashed line), ^{120}Sn + ^{40}Ar (short-dashed line). In each spectrum, the last point corresponds to 25% feeding (correction of a factor of 4). The thin solid line is a plot of $\mathcal{J}^{(2)}_{band}$ for ^{124}Sn + ^{40}Ar.

suggests it is due to alignment effects. The comparison with the $\mathcal{J}^{(2)}_{eff}$ spectrum of its isotone ^{162}Yb further suggests[8] that this is a proton alignment of $h_{9/2}$, $i_{13/2}$ orbitals which come down to the Fermi level (see Figure 5) around $\hbar\omega \sim 0.6$ MeV for Er nuclei.

The $\mathcal{J}^{(2)}_{eff}$ spectra for ^{158,156}Er illustrate Fermi level and shape effects. As the neutron Fermi level goes down in that region it comes closer to the highly aligned $\Omega = 1/2$ components of the intruder $i_{13/2}$ neutron subshell, and the nucleus becomes less deformed. Both these reasons make the valence shell backbends (hole-backbends) easier. This is what we see in the lower frequency region: in the lighter nuclei, the valence backbends are compressed in frequency which makes the lower peak taller and narrower than in the heavier nuclei. At higher frequencies, where particle alignments are expected, the Fermi level effect just described would be opposite (i.e., alignments would be delayed) for particle type backbend (like $h_{9/2}$, $i_{13/2}$ proton backbends) coming from the next shell. Although the proton Fermi level does not change from ^{160}Er to ^{156}Er the latter is softer and might generate high spins more efficiently by acquiring large deformations. This would also produce high values of $\mathcal{J}^{(2)}_{eff}$. We think this deformation effect might be happening in ^{156}Er.

5. FUTURE PROSPECTS

Although continuum γ-ray studies begin to reveal rather fine details like single-particle effects, a much better understanding of nuclear structure at high spins would be achieved if those spectra could be resolved. With recent progress in technology, there is indeed a hope to resolve several bands up to spin around 50 $\hbar$.

The idea is to build large arrays of Compton-suppressed Ge detectors. The Compton suppression improves greatly the peak to background ratio, the more gain the higher the coincidence order. Large arrays produce high rates and therefore open the possibility of recording higher order coincidences. Multiple coincidences increase the number of "resolvable points:" for example, if there are N resolvable points in a given energy interval of a single spectrum, there will be N^3 such points in a triple coincidence spectrum. Also triple coincidences can be used to make double gates, with which more bands can be separated, since each band is now characterized by two transitions instead of one.

In Berkeley, we are building an array of 21 Compton-suppressed Ge detectors. They are placed on three rings around a target and the central one is shown in Figure 8. This was possible because of the small size (~12.5 x 12.5 cm) of the suppressors which are made of Bismuth Germanate, a scintillator material, twice as dense as sodium iodide, and recently available in large sizes. With such a system, the peak to total ratio (counted from 300 KeV up) for a 1 MeV γ-ray is about 50%. We estimate that using triple concidences we will be able to separate ten times more bands than we can with only double coincidences.

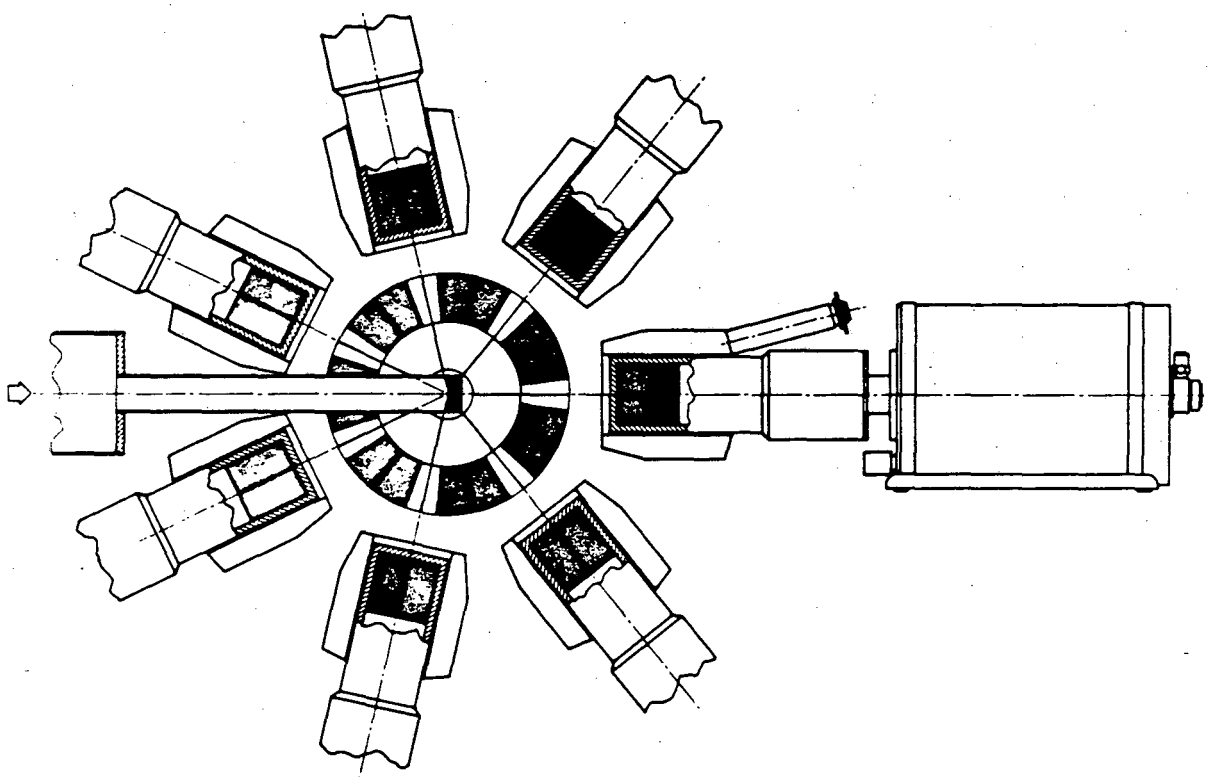

FIGURE 8
Cross-section of the central ring of seven Compton-suppressed germanium detectors. The beam comes from the left and the target is in the center. Also shown is the cross-section of a central Bismuth-germanate ball.

6. CONCLUSION

Continuum γ-ray studies have considerably enriched our knowledge of high spin properties of the nucleus. They lead to new concepts like the existence of several moments of inertia and their relation to single particle and collective effects. The results suggest that single particle effects may be identified at the highest spins. But only qualitative trends can be measured with such methods. More quantitative spectroscopy will require resolving the spectra, which we hope to accomplish up to spin around 50 $\hbar$ in the near future.

The results already obtained in Daresbury with the first Compton-suppressed array show exciting possibilities.

ACKNOWLEDGEMENT

This work has been done in collaboration with colleagues and visitors. I would like to thank them and especially R.M. Diamond and F.S. Stephens. This work was supported by the Director, Office of Energy Research, Division of Nuclear Physics of the Office of High Energy and Nuclear Physics of the U.S. Department of Energy under Contract No. DE-AC03-76SF00098.

REFERENCES

1) S. Cohen, F. Plasil and W.J. Swiatecki, Ann. Phys. 82 (1974) 557.
2) J.O. Newton et al., Phys. Rev. Lett. 38 (1977) 810.
3) R.M. Diamond and F.S. Stephens, Ann. Rev. Nucl. Part. Sci. 30 (1980) 85.
4) G. Andersson et al., Nucl. Phys. A268 (1976) 205.
5) A. Bohr and B.R. Mottelson, Nuclear Structure, Vol. 2 (W.A. Benjamin, Reading, 1975).
6) M.A. Deleplanque et al., Phys. Rev. Lett. 45 (1980) 172.
7) P.J. Nolan, Phys. Lett. 128B (1983) 285.
8) M.A. Deleplanque et al., Phys. Rev. Lett. 50 (1983) 409.

TECHNICAL INFORMATION DEPARTMENT
LAWRENCE BERKELEY LABORATORY
UNIVERSITY OF CALIFORNIA
BERKELEY, CALIFORNIA 94720